Mon. Not. R. astr. Soc. (1980) **191**, 887–896

The large-scale structure of X-ray clusters of galaxies – II

P. E. J. Nulsen and A. C. Fabian *Institute of Astronomy, Madingley Road, Cambridge CB3 0HA*

Received 1979 November 9; in original form 1979 September 14

Summary. Scanning data from the A-2 experiment on *HEAO-1* are used to investigate the large-scale structure of the gas distribution within eight well observed X-ray clusters. A large ($\sim 1^\circ$) halo of weak X-ray emission is found around the Perseus cluster and fitted to a hydrostatic polytropic model for the gas distribution.

For the eight remaining clusters, constraints are placed on the range of such models which are consistent with the data. In particular the expected microwave dip is typically limited to $\Delta T/T \lesssim 10^{-4}$.

1 Introduction

Most X-ray observations of the intracluster gas in clusters of galaxies are dominated by emission from the core regions (radii $\lesssim 1$ Mpc). This is largely due to the dependence of the thermal X-ray emissivity upon the square of the gas density. The data do not in general justify being modelled by any more than a few parameters, such as those of a hydrostatic atmosphere of polytropic gas. The *Uhuru* data on the Coma cluster, for example, have been used by Lea (1975) to fit hydrostatic polytropes that are just bound (i.e. zero temperature at infinity) and by Cavaliere & Fusco-Femiano (1976) for more general temperatures and cluster potentials. Gull & Northover (1975) have considered adiabatic atmospheres for the Coma and Perseus clusters. In these models most of the mass of intracluster gas is inferred to lie in the outer regions of the clusters, where it is relatively difficult to study owing to its low surface brightness.

Here we present the results of fitting general hydrostatic polytropic models to the X-ray emission within 40 core radii of eight clusters of galaxies scanned by the A-2 experiment (a collaborative effort led by E. Boldt of GSFC and G. Garmire of CIT with collaborators at GSFC, CIT, JPL and UCB; Rothschild *et al.* 1978) on the *HEAO-1* satellite. This experiment has good sensitivity for our purposes owing to its low internal background. It operates over a higher energy range (3–30 keV) than that of the Einstein Observatory (0.2–3 keV; Giacconi *et al.* 1979) from which much higher resolution X-ray images of clusters will be forthcoming. The A-2 experiment consists of six multiwire gas-proportional-counters pointing perpendicular to the spin axis of the spacecraft. We use data from two of

these detectors, one operating at medium X-ray energies (MED) and the other with a response at higher energies (HED3). The relatively large fields of view ($3° \times 3°$ and $3° \times 1°.5$ FWHM for each detector) mean that our results apply to structure in clusters on the size of $\sim 1°$. We have previously used these data to search for evidence of large haloes around clusters as reported by Forman *et al.* (1978). Our results (Nulsen *et al.* 1979) were incompatible with such haloes and provided limits on simple geometrical profiles for the emission. The Perseus cluster was the only one to show evidence for extension on the order of $1°$. We clarify here the structure of this low-surface-brightness emission and place useful limits on the state of the gas in the seven other clusters, including the Coma cluster. The results enable us to place limits on the expected microwave dip in these clusters (Lake & Partridge 1979; Birkinshaw, Gull & Northover 1978).

2 Description of the models

We assume that the intracluster gas may be treated as a hydrostatic polytrope confined by a spherically symmetric self-gravitating mass distribution:

$$\rho(r) = \begin{cases} \rho_0(1 + r^2/r_c^2)^{-3/2}, & r \leqslant r_c \\ \rho_0 2^{-3/2}(r/r_c)^{-a}, & r > r_c. \end{cases} \tag{1}$$

The core radius, r_c, is set equal to 250 kpc (Bahcall 1977) when comparing the model with data. ρ_0 is the central density and a is a free parameter in the range $2 \lesssim a \lesssim 3$ (Rood *et al.* 1972; van den Bergh 1977). This mass distribution defines a gravitational potential:

$$\phi(r) = 4\pi G\rho_0 r_c^2 f(r/r_c) \tag{2}$$

where

$$f(x) = \begin{cases} 1 - x^{-1}\ln(x + \sqrt{1+x^2}), & x \leqslant 1 \\ (x^{2-a} - 1)/[2^{3/2}(2-a)(3-a)] + \{\ln(1+\sqrt{2}) - 1/\sqrt{2} - 1/[2^{3/2}(3-a)]\} \\ \quad \times (1 - x^{-1}) + 1 - \ln(1+\sqrt{2}), & x > 1. \end{cases} \tag{3}$$

The gas has a polytropic index $\gamma (p \propto \rho^\gamma)$ with $\gamma \leqslant 5/3$ for convective stability. The gas temperature T is then given by

$$\frac{T}{T_0} = 1 - \frac{(\gamma - 1)\,\mu m_H \phi}{\gamma k T_0} \tag{4}$$

and the number density, n, by

$$\frac{n}{n_0} = \begin{cases} (T/T_0)^{1/(\gamma-1)}, & \gamma \neq 1 \\ \exp(-\mu m_H \phi/kT_0), & \gamma = 1. \end{cases} \tag{5}$$

where T_0 and n_0 are the central gas temperature and density, respectively; μm_H is the mean mass per particle. Following Cavaliere & Fusco-Femiano (1976) we introduce the parameter

$$\tau = \mu m_H v_\parallel^2/kT_0,$$

where $v_\parallel$ is the line-of-sight velocity dispersion of the cluster. Equation (4) then becomes

$$\frac{T}{T_0} = 1 - \frac{(\gamma - 1)}{\gamma}\kappa\tau f\left(\frac{r}{r_c}\right), \tag{6}$$

where $\kappa = 4\pi G\rho_0 r_c^2/v_\parallel^2$ and determines the dynamics of the self-gravitating cluster. The approximate isothermal nature of clusters (Gregory 1975) suggests that $\rho(r)$ should have the same form as $n(r)$ given by equation (5), with $\gamma, \tau = 1$ (Cavaliere & Fusco-Femiano 1976). κ can then be determined by requiring that $n(r) \simeq$ constant $\rho(r)$ in equation (1). We find that a value of $\kappa \simeq 9$ gives a reasonable agreement between these profiles and is the value adopted.

The procedure used here to determine κ relies on the assumption that the cluster potential is well represented by a self-gravitating, isothermal sphere. The velocity distribution should then be locally isotropic and the velocity dispersion constant throughout the cluster. The isothermal King (1966) model is often used to interpret optical cluster observation and would give a similar value for κ. It can also explain, for example, the slight radial gradient in velocity dispersion observed in the Coma cluster (Rood *et al.* 1972). However, use of this model is not justified in clusters which have only collapsed recently, or are still collapsing (e.g. Gott & Rees 1975), and which are certainly not tidally limited. It is then likely that galaxy motions away from the core are anisotropic with radial motions dominant (White 1976; Visvanathan & Sandage 1977). This results in κ being overestimated. Fortunately, in our empirical models for the gravitating matter distribution, $\kappa\tau$ determines the gas distribution. Thus to change κ it is only necessary to rescale any results in τ.

We note that many clusters do not appear to be spherical (Bahcall 1974; Binney 1977). This need not invalidate our assumptions since the cluster potential, and thus gas distribution, remain reasonably spherically symmetric (Binney & Strimpel 1978).

Since we are only interested in the emission profile, one of our models is fully described by the parameters γ, τ, a and T_0. This last parameter only enters through the spectral response of the detectors which is fairly flat for thermal bremsstrahlung from a gas with $3 \lesssim kT \lesssim 30$ keV. Our results are thus not sensitive to $T_0 > 3$ keV, and we fix $kT_0 =$ 10.4 keV in much of what follows. It should be noted, however, that $\tau \propto T_0^{-1}$ for a given $v_\parallel$ when considering a particular cluster. Our parameters relate to T_∞ of Gull & Northover (1975), and $\alpha = T_\infty/T_0$ of Sarazin & Bahcall (1977) by

$$T_\infty = T_0\left[1 - \frac{(\gamma-1)}{\gamma}\kappa\tau f(\infty)\right]$$

$$= T_0\left[1 - \frac{(\gamma-1)}{\gamma}9\tau\left(1 - \frac{5-2a}{2^{3/2}(2-a)}\right)\right].$$

3 Results for Perseus

A grid of the above models, for various γ and τ and for $a = 2.5$ and 2.7, was convolved with the effective collimator and spectral responses for the MED and HED3. These were fitted to 100 bins of scanning data about the Perseus cluster by varying the source and background intensities until χ^2 was minimized. The source position was determined by fitting a point source to the data.

The minimum χ^2 values, listed in Table 1, show a marked improvement over the corresponding values for a point source. The 50 innermost data points and the best-fitting model ($\gamma = 1.25$, $\tau = 0.68$ and $a = 2.7$) are displayed in Fig. 1. We have subtracted the best-fitting point source response from both data and model in order to make the small residuals easily visible. In Fig. 2 we have plotted the temperature and density as a function of r for this model. The improvement in χ^2 is due to the presence of a weak halo of emission $\sim 1^\circ$ in size around the cluster.

Table 1. Column 3 shows χ^2 for the models best fitting the data for the Perseus cluster ($kT_0 = 10.4$ keV) and column 4 shows χ^2 for the best-fitting point source to the same data.

Detector	a	Best fit χ^2	Point source χ^2
MED	2.5	134.22	177.11
MED	2.7	133.63	
HED3	2.5	130.35	211.81
HED3	2.7	129.82	

Ninety per cent confidence contours for γ and τ are plotted in Fig. 3(a and b). There is good agreement between the independent contours obtained for the MED and HED3, which strengthens our confidence in the results. The difference between these contours is due to the different spectral responses of the detectors. Combining the contours results in a very limited acceptable range for γ and τ.

No allowance has been made for the 'point' source at the cluster centre (Fabian *et al.* 1974; Gorenstein *et al.* 1978). This only affects our results slightly since the point source is a small fraction of the total cluster emission, most of which appears point-like to our detectors.

Because of the very steep dependence of the X-ray emission per unit volume on the temperature for low γ (since $n^2 \sim T^{2/(\gamma-1)}$), the observed cluster temperature, $T_x \simeq 6.8$ keV (Mushotzky *et al.* 1978), must be close to T_0. Also, since $\gamma > 1$, we always have $T_x < T_0$. Thus we can use the observed cluster velocity dispersion of 1420 km s^{-1} (taken from Mitchell *et al.* 1979) to get $\tau \lesssim 1.88$. This is about twice the acceptable values. The uncertainty in cluster dynamics, and thus κ, noted in Section 2 prevents us from drawing any firm conclusions from this discrepancy. Nevertheless, it highlights the fact that the observed extent of the cluster emission is larger than we would have expected on the basis of simple hydrostatic models. We should regard this result as showing that X-ray and optical observations of clusters taken together are now capable of providing more reliable information about the gravitating mass distribution in clusters than are optical observations alone (see, e.g. Binney & Strimpel 1978).

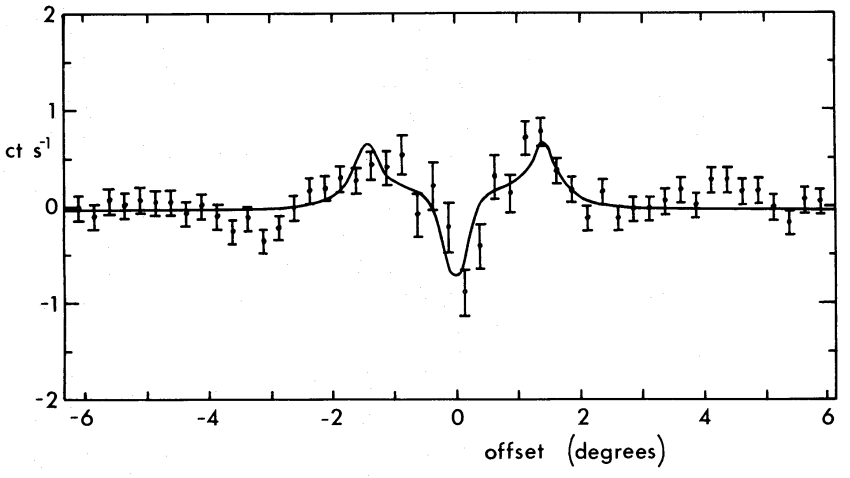

Figure 1. Predicted count rate for the best-fitting model (full curve: $\tau = 0.68$, $\gamma = 1.25$ and $a = 2.7$), after subtraction of a point source, plotted against scan distance from the centre of the Perseus cluster for HED3. The observed count rates are shown with 1σ error bars. The scan direction is approximately north–south.

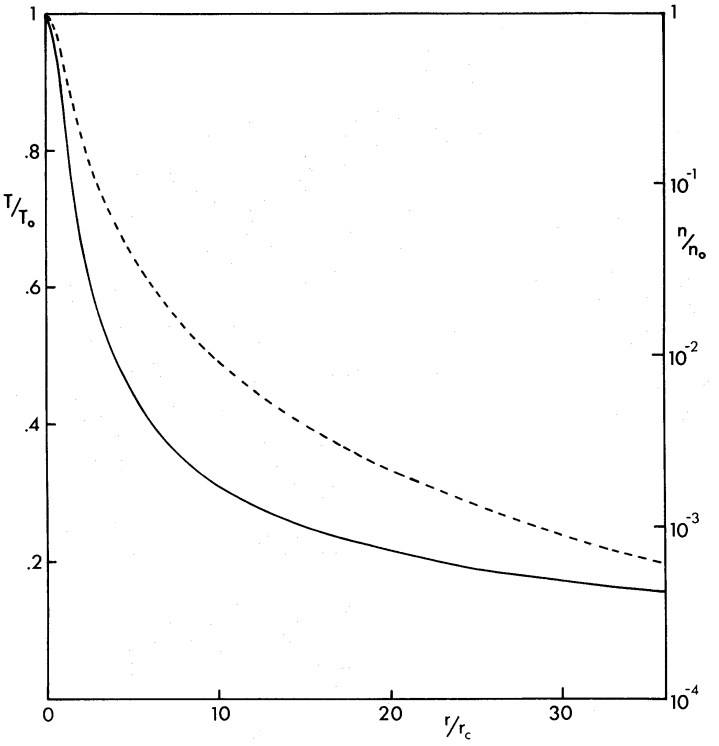

Figure 2. Temperature (full curve) and density (dashed curve) versus r/r_c for the best-fitting hydrostatic polytrope to the data for the Perseus cluster ($\tau = 0.68$, $\gamma = 1.25$ and $a = 2.7$). The left-hand scale refers to the temperature and the right-hand scale to the density.

It is quite remarkable that Gorenstein *et al.* (1978), fitting a slightly less general hydrostatic model to the central 20 arcmin in Perseus, found $\tau = 0.62 \pm 0.06$. This suggests that our best model may apply over a full decade in radius. There is at present no sound theoretical reason why a hydrostatic polytrope should provide a good fit throughout the cluster.

Finally, we note that the density of the position of NGC 1265 is about one-tenth of that at one core radius. This is roughly similar to that required to explain the form of the radio source 3C 83.1 (Begelman, Rees & Blandford 1979).

4 Results for the other sources

For the remaining cluster sources, limits can be placed on the acceptable range of γ and τ by comparing the expected ratios of the count rates in the 3° and 1°.5 fields of view with those measured in our earlier paper (Nulsen *et al.* 1979). The range of expected ratios is between 1.0 and 2.0 in principle, although in practice we would not expect to measure any greater than about 1.5, because extremely extended sources affect the background estimates. We truncate all atmospheres at 40 core radii, which corresponds to diameters $>4°$ in the most distant cluster considered here.

Near the values of γ and τ where this ratio differs significantly from unity (i.e. by a few per cent), it is very sensitive to γ and τ. This leads to the limits on the range of γ and τ obtained for the well-observed clusters (Table 2) being indistinguishable in Fig. 3(a and b). They are therefore indicated by a single line in each.

Table 2 lists some of the properties of these clusters (taken mainly from Mitchell *et al.* 1979). Included in the table are the 'observational' τ values obtained using the observed

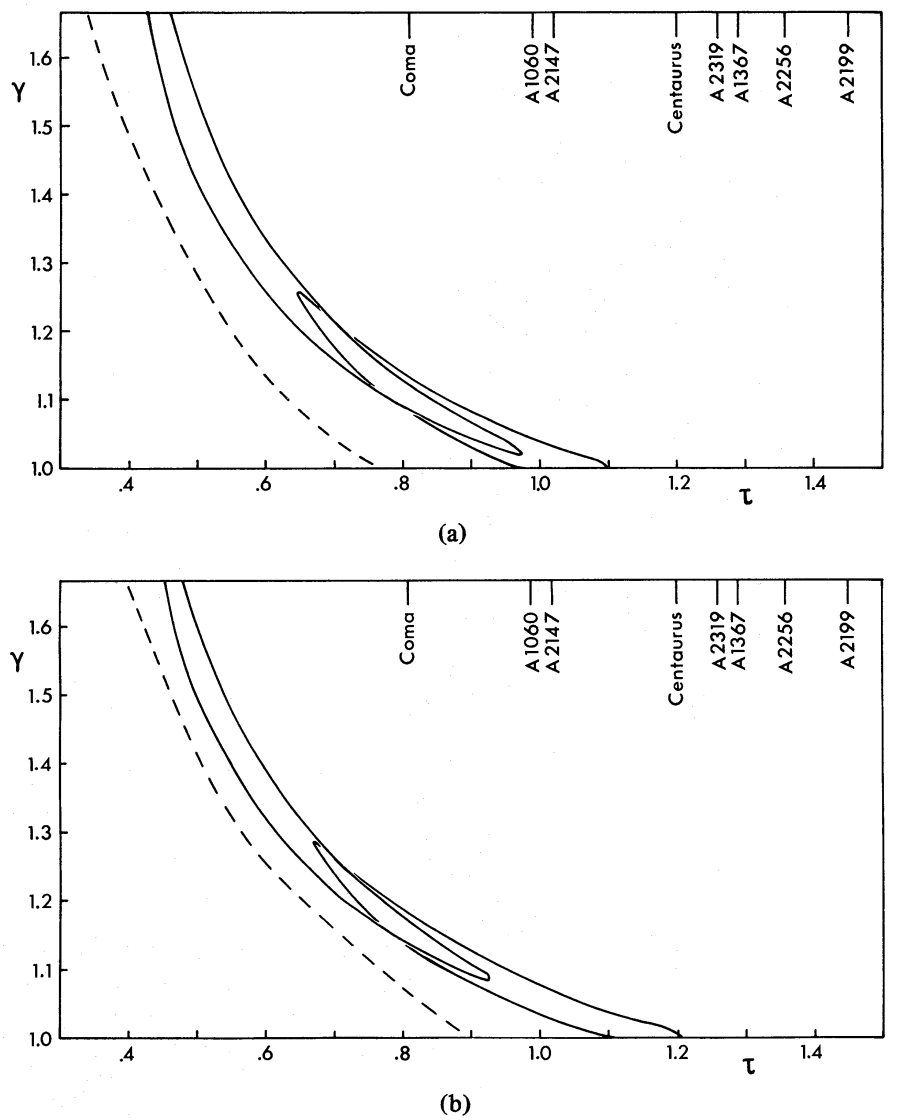

Figure 3. Limits on the range of γ and τ for the clusters listed in Table 2. In (a) $a = 2.5$ and in (b) $a = 2.7$. All of the observed clusters lie to the right of the dashed curve which is obtained using the measured $3° - 1°.5$ flux ratios in the MED. The τ values indicated by cluster names are the observational values (Table 2) and represent upper limits on τ. The full curves are 90 per cent confidence contours for the Perseus cluster for the MED (lower) and HED3 (upper) respectively.

cluster temperatures and velocity dispersions. Apart from the uncertainty in the τ scale in Fig. 3 (due to the uncertainty in κ), these may be regarded as upper limits on τ for the individual clusters (for $\gamma \geqslant 1$). Thus we have plotted them in Fig. 3 as such (ignoring the substantial error in most of the determinations).

As pointed out in the previous section, the sensitive dependence of the volume emissivity on T_0 causes the observed X-ray temperature to be close to T_0. Another constraint on T_0 (and thus τ) is the observation of Fe line emission from several clusters (Mushotzky *et al.* 1978; Mitchell *et al.* 1979). Since isothermal models give roughly cosmic Fe abundance, high values of T_0 ($kT_0 \gtrsim 15$ keV) would require unreasonably high Fe abundances (see, e.g. Bahcall & Sarazin 1978). This constrains the value of T_0 quite severely for clusters with 6.7-keV Fe emission, as do the results of Fig. 3, but the former constraint does not depend on the poorly-known cluster structure.

Table 2. Properties of eight well observed clusters (taken mainly from Mitchell *et al.* 1979 and Mushotzky *et al.* 1978). In column 2 is the redshift, column 3 the line-of-sight velocity dispersion in km s^{-1} and column 4 the observed cluster temperature kT_X in keV. The observational τ value (column 5) is $\mu m_H v_\parallel^2/kT_X$ and we note that this is not accurately determined for most clusters. In column 6 is the 3°–1°.5 flux ratio taken from Nulsen *et al.* 1979. In column 7 we list the X-ray luminosity of the clusters in units of 10^{45} erg s^{-1} and in column 8 the limit on $\Delta T/T$ determined by equation (9) in units of 10^{-4}.

Cluster	z	$v_\parallel$	kT_X	τ	R	L_X	Dip
A426	0.0182	1420	6.3	1.88	1.05±0.016	2.81	4.3
A1060	0.0112	771	3.5	0.99	0.89± 0.12	0.06	0.3
Centaurus	0.0109	870	3.7	1.20	1.10± 0.09	0.16	0.5
A1656	0.0232	909	6.0	0.81	0.98± 0.09	1.68	1.7
A2147	0.0374	1120	7.2	1.02	0.88± 0.17	0.73	1.6
A2199	0.0309	887	3.2	1.45	0.95± 0.12	0.47	0.9
A2256	0.0603	1274	7.0	1.36	0.96± 0.10	1.93	3.0
A2319	0.0564	1637	12.5	1.26	0.94± 0.05	3.67	6.1

The acceptable range of γ and τ does allow atmospheres with large-scale ($\sim 1°$) weak emission, but not the haloes of Forman *et al.* (1978). The limits in Fig. 3 are insensitive to the observed ratios of 3°–1°.5 count rates in the range 1–1.2, and to $kT_0 \gtrsim 3$ keV for nearby ($\lesssim 300$ Mpc) clusters. The overall limits on the ratio of 3°–1°.5 count rates for the 30 clusters considered in Nulsen *et al.* (1979) thus imply that nearly all clusters fall to the right of the limits indicated in Fig. 3.

We have not included the Virgo cluster in our analysis because of its irregular X-ray structure (Lawrence 1978).

5 Microwave dips

The limits on γ and τ from the previous section allow us to constrain the expected dips in the microwave background due to the Zel'dovich effect (Lake & Partridge 1977). In an atmosphere with a given n_0 and T_0 the maximum $\Delta T/T$ which is consistent with the constraints of Fig. 3 is

$$\frac{\Delta T}{T} \leqslant 10^{-4} T_8 n_{-3} r_{250}, \tag{7}$$

for $a = 2.5$, $\gamma = 5/3$ and $\tau = 0.35$, and where $T_0 = 10^8 T_8$ K, $n_0 = 10^{-3} n_{-3}$ cm^{-3} and $r_c = 250 r_{250}$ kpc. This limit is not affected by the uncertainty in κ and is insensitive to a. Bearing in mind the constraints on T_0 discussed above, for typical cluster parameters, the limit (7) is less than can be observed at present (Lake & Partridge 1979; Birkinshaw 1979). The dip for the best-fitting model for Perseus is

$$\frac{\Delta T}{T} = 5 \times 10^{-5} T_8 n_{-3} r_{250}, \tag{8}$$

for $a = 2.7$, $\tau = 0.68$ and $\gamma = 1.25$.

Well determined values of n_0 and T_0 are not yet available for any cluster. As an alternative to the limit (7), we can determine the maximum dip, subject to the constraints in Fig. 3, which can be produced by a cluster with a given X-ray luminosity and velocity dispersion. In this case the value of τ and $v_\parallel$ are used to determine T_0, so that the X-ray luminosity then determines n_0. The maximum dip is

$$\frac{\Delta T}{T} \leqslant 1.5 \times 10^{-4} L_{45}^{1/2} v_3^{3/2} r_{250}^{-1/2} \left(\frac{\kappa}{9}\right)^{3/4}, \tag{9}$$

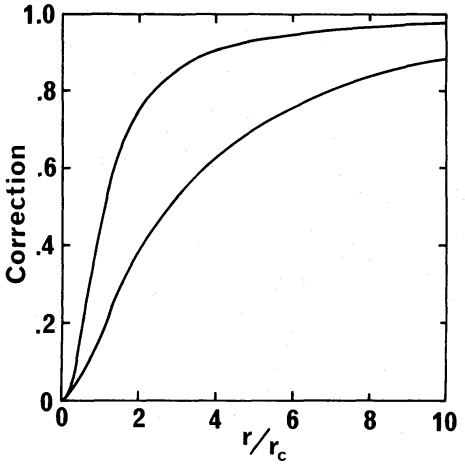

Figure 4. The correction to the limits on $\Delta T/T$ is shown as a function of the beam-throw in units of r_c. The lower curve applies to equation (7) and the upper to equations (8) and (9).

for $a = 2.5$, $\gamma = 1.1$ and $\tau = 0.85$, where the X-ray luminosity of the cluster is $10^{45} L_{45}\,\mathrm{erg\,s^{-1}}$ and $v_{\parallel} = 10^3 v_3\,\mathrm{km\,s^{-1}}$. The limits (9) are given in Table 2.

As a result of using $v_{\parallel}$ to determine T_0, these limits depend on the rather uncertain value of κ. For example, if we reduce κ to make the best-fitting τ for Perseus equal to the 'observed' value (Table 2), the limit (9) for Perseus becomes $\Delta T/T \lesssim 2 \times 10^{-4} r_{250}^{-1/2}$. We also note that this limit occurs for τ and γ well inside the acceptable range given in Fig. 3. Thus it is not an observational limit in the sense of equation (7) but is determined by the hydrostatic models we have used. This means that the data provide no new constraint when used in this way.

The microwave dip is generally measured as the difference between the value at the cluster centre and that for an annulus surrounding it. The radius of the annulus is typically only a few core radii, so that the measured dip is less than the total dip. This means that the limits discussed above must be reduced by a factor (Fig. 4) which depends on the radius of the annulus (beam-throw) used in a given measurement.

Clumping of the X-ray-emitting gas will reduce the expected dips for a given X-ray luminosity. Thus the only way to violate the constraints (7) and (9) is for the microwave dips to be produced by a high-temperature component of the gas which does not contribute significantly to the X-ray output of the cluster. In the region where the cooler gas occurs, the hot gas must have a comparable or lower pressure, and, since the dip is proportional to the line integral of the pressure, the constraints would still apply. In order to violate them the hot gas must also occur in a halo outside the X-ray-emitting gas. The lack of any such halo in the HED3 data requires a very low density for such gas, so that a very large volume of gas is required to produce a dip comparable to that given in equations (7) or (9). The resultant dip then has an angular size comparable to or greater than the cluster (*cf.* Lake & Partridge 1977; Birkinshaw, Gull & Northover 1978). We conclude that only very contrived models for the gas distribution in the clusters of Table 2 can violate the constraints given by equations (7) and (9).

6 Discussion

The constraints on the acceptable range of hydrostatic models in Fig. 3 allow us to limit the total mass of gas in these clusters. However, in general the mass limits are not useful as they

exceed the cluster virial masses. For the best-fitting model for Perseus ($\tau = 0.68$, $\gamma = 1.25$ and $a = 2.7$), the total mass within 40 core radii is $1.8 \times 10^{14} n_{-3} M_{\odot}$. This is $\sim 5 n_{-3}$ per cent of the virial mass for Perseus (Bahcall 1974), and a large fraction of the gas lies well outside the cluster core (see Fig. 2). Thus we may describe this gas as forming a halo around the Perseus cluster. We emphasize that this is a much smaller effect than that reported by Forman *et al.* (1978) for eight other clusters, and that their conclusions are not consistent with our data (Nulsen *et al.* 1979; Pravdo *et al.* 1979).

The hydrostatic polytrope used to fit the data is simply a model for the X-ray emission profile for Perseus. The best-fitting density and temperature profiles of Fig. 2 are thus not determined very reliably. In particular, since the sensitivity of the detectors drops sharply for $kT \lesssim 1.5$ keV, we see no emission from $r \gtrsim 15 r_c$ (i.e. $\gtrsim 2^{\circ}$ from the cluster centre) so that the data do not require any gas at these distances. The model surface-brightness at $r = 15 r_c$ is about 10^{-4} of that at $r = r_c$, so that it would be extremely difficult to detect. If the gas is sufficiently clumped, the emission may be detectable with the Einstein Observatory. In that case the limits on the mass of gas and the microwave dip due to Perseus could be greatly reduced.

The discrepancy between the observed and fitted values for τ in the Perseus data may be regarded as confirmation of the uncertainty in cluster dynamics as determined by optical observations. Uncertainty in the determination of cluster core radii (e.g. Quintana 1979) or even their meaning, the lack of knowledge about galaxy motions in the plane of the sky, and the indeterminate distances of galaxies allow a great deal of freedom in models of cluster dynamics. These uncertainties enter our models principally through the parameter κ and can be corrected, if necessary, by rescaling τ.

7 Conclusions

We have used scanning data from the A-2 experiment on *HEAO-1* to constrain the large-scale structure of the gas distribution within eight well-observed X-ray clusters. We find a large ($\sim 1^{\circ}$) halo of weak X-ray emission around the Perseus cluster which we fit to hydrostatic, polytropic models for the gas distribution. The best-fitting models indicate a ratio of velocity dispersion to gas temperature significantly lower than that derived directly from the observed values. This suggests that the cluster mass distribution is not well described by the simple models used here. The discrepancy may be due to asphericity, local anisotropy of the velocity distribution or to departures from equilibrium.

For the seven remaining clusters we find useful constraints on the range of such models which are consistent with the observations. In particular we find that the microwave dip expected in these clusters is typically $\Delta T/T \lesssim 10^{-4}$ (see equation 7).

Acknowledgments

We are grateful to Dr Elihu Boldt and his colleagues at Goddard Space Flight Center for their help. PEJN acknowledges receipt of an Isaac Newton Studentship. ACF acknowledges the Radcliffe Trust for support.

References

Bahcall, J. N. & Sarazin, C. L., 1978. *Astrophys. J.*, **219**, 781.
Bahcall, N. A., 1974. *Astrophys. J.*, **187**, 439.
Bahcall, N. A., 1977. *A. Rev. Astr. Astrophys.*, **15**, 505.
Begelman, M. C., Rees, M. J. & Bandford, R. D., 1979. *Nature*, **279**, 770.
Binney, J., 1977. *Astrophys. J.*, **215**, 492.

Binney, J. & Strimpel, O., 1978. *Mon. Not. R. astr. Soc.*, **185**, 473.
Birkinshaw, M., 1979. *Mon. Not. R. astr. Soc.*, **187**, 847.
Birkinshaw, M., Gull, S. F. & Northover, K. J. E., 1978. *Mon. Not. R. astr. Soc.*, **185**, 245.
Cavaliere, A. & Fusco-Femiano, R., 1976. *Astr. Astrophys.*, **49**, 137.
Fabian, A. C., Zarnecki, J. C., Culhane, J. L., Hawkins, F. J., Peacock, A., Pounds, K. A. & Parkinson, J. E., 1974. *Astrophys. J. Lett.*, **189**, L59.
Forman, W., Jones, C., Murray, S. & Giacconi, R., 1978. *Astrophys. J. Lett.*, **225**, L1.
Giacconi, R., Branduardi, G., Briel, U., Epstein, A., Fabricant, D., Feigelson, E., Forman, W., Gorenstein, P., Grindlay, J., Gursky, H., Harnden, F. R., Henry, J. P., Jones, C., Kellogg, E., Koch, D., Murray, S., Schreier, E., Seward, F., Tananbaum, H., Topka, K., Van Speybroeck, L., Holt, S. S., Becker, R. H., Boldt, E. A., Serlemitsos, P. J., Clark, G., Canizares, C., Markert, T., Novick, R., Helfand, D. & Long, K., 1979. *Astrophys. J.*, **230**, 540.
Gorenstein, P., Fabricant, D., Topka, K., Harnden, F. R. & Tucker, W. H., 1978. *Astrophys. J.*, **224**, 718.
Gott, J. R. & Rees, M. J., 1975. *Astr. Astrophys.*, **45**, 365.
Gregory, S. A., 1975. *Astrophys. J.*, **199**, 1.
Gull, S. F. & Northover, K. J. E., 1975. *Mon. Not. R. astr. Soc.*, **173**, 585.
King, I. R., 1966. *Astr. J.*, **71**, 64.
Lake, G. & Partridge, R. B., 1977. *Nature*, **270**, 502.
Lake, G. & Partridge, R. B., 1979. Preprint.
Lawrence, A., 1978. *Mon. Not. R. astr. Soc.*, **185**, 423.
Lea, S. M., 1975. *Astrophys. Lett.*, **16**, 1.
Mitchell, R. J., Dickens, R. J., Bell Burnell, S. J. & Culhane, J. L., 1979. *Mon. Not. R. astr. Soc.*, **189**, 329.
Mushotzky, R. F., Serlemitsos, P. J., Smith, B. W., Boldt, E. A. & Holt, S. S., 1978. *Astrophys. J.*, **225**, 21.
Nulsen, P. E. J., Fabian, A. C., Mushotzky, R. F., Boldt, E. A., Holt, S. S., Marshall, F. J. & Serlemitsos, P. J., 1979. *Mon. Not. R. astr. Soc.*, **189**, 183.
Pravdo, S. H., Boldt, E. A., Marshall, F. J., McKee, J., Mushotzky, R. F., Smith, B. W. & Reichert, G., 1979. *Astrophys. J.*, **234**, 1.
Quintana, H., 1979. *Astr. J.*, **84**, 15.
Rood, H. J., Page, T. L., Kintner, E. C. & King, I. R., 1972. *Astrophys. J.*, **175**, 627.
Rothschild, R., Boldt, E., Holt, S., Serlemitsos, P., Garmire, G., Agrawal, P., Riegler, G., Bowyer, S. & Lampton, M., 1978. *NASA Technical Memorandum 79574.*
Sarazin, C. L. & Bahcall, J. N., 1977. *Astrophys. J. Suppl.*, **34**, 451.
van den Bergh, S., 1977. *Vistas Astr.*, **21**, 71.
Visvanathan, N. & Sandage, A., 1977. *Astrophys. J.*, **216**, 214.
White, S. D. M., 1976. *Mon. Not. R. astr. Soc.*, **177**, 717.